SenSation :A New 2 DOF Parallel Mechanism for a Haptic Device

*^Young-Hoon Chung , *JungHoon Choo, **Jae-Won Lee**

Graduate School of Mech. Eng. of Yeungnam Univ.*^ ' * *^ E-mail : parallel_robot@yahoo.co.kr
Mechanical Engineering of Yeungnam Univ.**, ** E-mail : jwlee@yu.ac.kr
Robotics Lab, Dept. of Mech. Eng., Yeungnam University, 214-1, Daedong, Kyongsan, Kyongbuk, 712-749, South Korea

Abstract

We propose a new two-degree of freedom parallel mechanism, the *SenSation*. The *SenSation* is designed in order to improve the kinematic performace and to achieve static balance. We use the pantograph mechanisms in order to change the location of active joints, which leads to transform a direct kinematic singularities into a non-singularities. The direct kinematic singular configurations of the *SenSation* occur near the workspace boundary, which means that we do not any more suffer from the singular configuration which occurs at the inside of workspace. Hence, the proposed mechanism can overcome disadvantage such as the singular configurations existing in the inside of workspace for a typical parallel mechanisms.

Using the property that position vector of rigid body rotating about a fixed point is normal to the velocity vector, Jacobian matrix is derived. Using the vector method, two different types of singularities of the *SenSation* can be identified and we discuss the physical significance of each of the three types of singularities. We will compare the kinematic performace of the *SenSation* with that of five-bar parallel mechanism. By specifying that the potential energy be fixed, the conditions for the static balancing of the *SenSation* is derived. The static balancing is accomplished by changing the center of mass of the links.

1. Introduction

Nowadays, the structure of mechanism has been changed from an open kinematic chain to a closed kinematic chain.

There are many examples of parallel mechanisms using a closed kinematic chain. Because of the high mechanical stiffness, low inertia, wide bandwidth, and the excellent load/weight ratio, the parallel mechanism is used in many industrial applications. In the field of robotics, the task required of the high speed and accuracy can be performed by virtue of parallel robots employing parallel mechanism. Parallel robots have induced numerous research activities in the Academic community for many years.

From the first parallel robot proposed by Gough[1] and Stewart[2], a lot of parallel robots or design methods have been studied. In the late 80's, a new field of both research and applications has been opened by Clavel[3] who developed the famous Delta manipulator which has the ability to move in high speed(30G). Recently, the machine-tool industry discovered the potential advantages of parallel mechanisms and most major machine-tool companies are in the process of extensive tests and evaluation of their parallel machines for 5-axis milling(Gidding&Lewis, Toyoda, Hexel, Ingersoll), for drilling tasks(Hitachi), for 3-axis milling tasks(Honda) [5][6][7]. Even if a lot of parallel mechanisms have been proposed, almost the 6 dof parallel mechanisms have been studied. However, in several applications, a 6 dof mechanism is not required and robots which have less than 6 dof can be used[8].

A parallel mechanism typically consists of moving platform that is connected to a fixed based by several limbs or legs. Typically, the limb(or leg) that composes the parallel mechanism such as type of the Delta and Stewart manipulator has the serial structure. If the limb is constructed by simple parallel mechanism, a parallel mechanism will have the better kinematic and dynamics performance than the parallel mechanism mentioned above. Hudgens and Tesar [9] employed the four-bar linkage as the limb of parallel mechanism. The platform motion is obtained by driving the input links of four-bar linkage, which are used to the mechanical advantages and to improve positional resolution of the mechanism, and F. tahmasebi[10] designed a 6 dof parallel manipulator by employing 2 dof five-bar linkage and then improved the positional resolution, stiffness and force control of the manipulator. Also, Antonio Frisoli [11][12] developed a novel tendon driven five-bar linkage with a large isotropic workspace and applied it to limbs of 6 dof haptic device, and then the device had a good the kinematic isotropy and the acceleration capability.

All previous research on design of parallel mechanism or manipulators relates to analyzing and optimizing the kinematic geometry without regard to the form of actuation of the joints. However, J.W.Kim and F.C.Park[13] illustrated the example that the location of actuators effects on the manipulability ellipsoid(see Fig.2 of paper[13]).

In this paper, we propose a new two-degree-of-freedom parallel mechanism, the *SenSation* that is intended for a good kinematic performance and static balance.

By using the property that position vector of rigid body rotating about a fixed point is normal to the velocity vector, Jacobian matrix is derived. By using the vector method, two different types of singularities of the *SenSation* can be identified and we discuss the physical significance of each of the two types of singularities.

We use the pantograph mechanisms in order to change the location of actuations, which lead to transform a direct singular configuration into a non-singular one. In section 4, we will show that the direct kinematic singularities of the proposed mechanism occur near the workspace boundary. We wil compare the kinematic performace of the *SenSation* with that of five-bar parallel mechanism[19].

We will derive the condition that the *SenSation* has zero-potential energy for all configurations.

2. Description of the *SenSation*

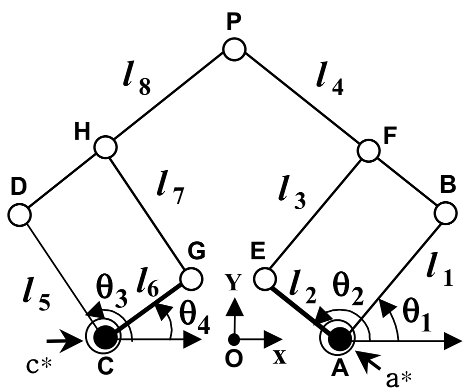

Figure 1. Schematic diagram of the *SenSation* and its coordinate system

The *SenSation* including two pantograph mechanisms consists of four revolute joints(**A,C,a*,c***) attached to the base, and seven revolute joints, eight links. The joint **a*** and **c*** is attached to the link **AB** and **CD** respectively, and the joint **A** and **C** is attached to the link **AE** and **CG** respectively. The distance between joint **A** and **C** is d. The global fixed coordinate frame{**O**} is located at point O, the middle of between joint **A** and **C**(see Fig. 1). The output is the joint **P** as shown in Fig.1.

Two motors are attached to the joint **A** of link **AE** and **C** of link **CG** respectively. When input links **AE** and **CG** rotate about joint **A** and **C** respectively, the links **BP** and **DP** have also the same rotation angle as input links **AE** and **CG** rotate respectively. Therefore, the joint **B** and **D** are also active joints, which lead to transform the direct kinematic singular configuration into non-singular one.

The *SenSation* has translational two-degree of freedom, as can be shown by applying the mobility criterion presented in Hunt[20]:

$$\boldsymbol{M} = 3(\boldsymbol{n} - \boldsymbol{j} - 1) + \sum_{\boldsymbol{i}=1}^{\boldsymbol{j}} \boldsymbol{f_i} \tag{1}$$

where $\boldsymbol{M}$ is the degree of freedom of mechanisms, $\boldsymbol{n}$ is the number of bodies in the mechanism, $\boldsymbol{j}$ is the number of joints and $\boldsymbol{f_i}$ is the number of degree of freedom of $\boldsymbol{i}$-th joint.

For the *SenSation*, $\boldsymbol{n}$ =9, $\boldsymbol{j}$ =11 and $\boldsymbol{f_i}$ =1 for each of the revolute joints. Application of Eq. (1) yields

$$\boldsymbol{M} = 3(9 - 11 - 1) + 11 = 2 \tag{2}$$

3. Kinematic Analysis

3.1 Inverse Kinematics

For the inverse kinematics, P_x, P_y are given, and the active joint angles θ_2, θ_4 ,are to be found. This can be can be accomplished on a sub-chain(**O→C→D→P**) by sub-chain (**O→A→B→P**). Figure 2 shows the link lengths and joint angles for a right sub-chain(**O→A→B→P**).

Referring to Fig. 2, the orign of the fixed coordinate frame is located at point **O**. The x-axis points along the direction of $\overrightarrow{\boldsymbol{OA}}$, the y-axis is perpendicular to $\overrightarrow{\boldsymbol{OA}}$. The distance between **O** and **A** is d/2.

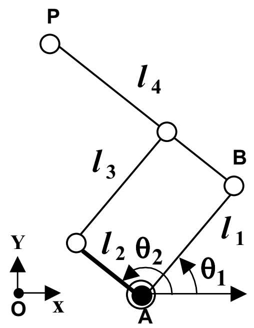

Figure 2. A right sub-chain of the *SenSation*.

From the geometry of Fig. 2, a vector-loop equation can be written as

$$\overrightarrow{\boldsymbol{OP}} = \overrightarrow{\boldsymbol{OA}} + \overrightarrow{\boldsymbol{AB}} + \overrightarrow{\boldsymbol{BP}} \tag{3}$$

Expressing the vector-loop equation above in the global fixed coordinate frame $\{\mathbf{O}\}$ gives

$$\begin{aligned} P_x &= \frac{d}{2} + l_1 C_1 + l_4 C_2 \\ P_y &= 0 + l_1 S_1 + l_4 S_2 \end{aligned} \tag{4}$$

Since θ_1 is a passive joint angle, it should be eliminated from the equation above. Toward this goal, we write Eq. (4) in the following form:

$$\begin{aligned} P_x - (\frac{d}{2} + l_4 C_2) &= l_1 C_1 \\ P_y - l_4 S_2 &= l_1 S_1 \end{aligned} \tag{5}$$

Summing the squares of two equations in (5) yields

$$(P_x - d/2 - l_4 C_2)^2 + (P_y - l_4 S_2)^2 - l_1^2 = 0 \tag{6}$$

We can arrange Eq.(6) in the following form:

$$\alpha_1 C_2 + \beta_1 S_2 + \lambda_1 = 0 \tag{7}$$

where, $\alpha_1 = -2(P_x - d/2) l_4$, $\beta_1 = 2 P_y l_4$,
$\gamma_1 = (P_x - d/2)^2 + P_y^2 + l_4^2 - l_1^2$

Substituting the trigonometric identities

$$\mathbf{cos}(\theta_2) = \frac{1-u_1^2}{1+u_1^2}, \mathbf{sin}(\theta_2) = \frac{2u_1}{1+u_1^2}, \text{ where, } \mathbf{tan}\left(\frac{\theta_2}{2}\right) = u_1$$

into Eq.(7), we obtain

$$(\gamma_1 - \alpha_1) u_1^2 + 2\beta_1 u_1 + (\gamma_1 + \alpha_1) = 0 \tag{8}$$

Solving Eq.(8) for $\boldsymbol{u}_1$ yields

$$u_1 = \frac{-\beta_1 \pm \sqrt{\beta_1^2 - (\gamma_1^2 - \alpha_1^2)}}{\gamma_1 - \alpha_1} \tag{9}$$

and

$$\theta_2 = 2\,\mathbf{tan}^{-1}\left(\frac{-\beta_1 \pm \sqrt{\beta_1^2 - (\gamma_1^2 - \alpha_1^2)}}{\gamma_1 - \alpha_1} \right) \tag{10}$$

Hence, corresponding to each given point **P** location, there are generally two solutions of θ_2 and two configurations of a right sub-chain. When Eq.(8) yields a double root, the two links **AB** and **BP** are in a fully stretched-out or folded-back configuration called the singular configuration. When Eq.(8) yields no real root, the specified point **P** location is not reachable. Following the same procedure, another sub-chain(O→C→D→P). configuration can be solved. We conclude that, in general, there are a total of four possible postures corresponding to a given point P location.

3.2 Jacobian Matrix

For the *SenSation*, the input vector is $\vec{\boldsymbol{\theta}}_{\boldsymbol{a}} = [\theta_2 , \theta_4]^{\mathbf{T}}$ and the output vector is $\overrightarrow{\boldsymbol{OP}} = [P_x , P_y]^{\mathbf{T}}$. A loop-closure equation can be written for each sub-chain. For a right sub-chain, we have

$$\overrightarrow{\boldsymbol{OP}} = \overrightarrow{\boldsymbol{OA}} + \overrightarrow{\boldsymbol{AB}} + \overrightarrow{\boldsymbol{BP}} \tag{11}$$

The angular velocity vectors of all links point in the positive z-direction as shown in Fig.1. A velocity vector- loop equation is obtained by taking the derivative of Eq.(11) with respect to time:

$$\dot{\overrightarrow{\boldsymbol{OP}}} = \dot{\theta}_1 \vec{\boldsymbol{k}} \times \overrightarrow{\boldsymbol{AB}} + \dot{\theta}_2 \vec{\boldsymbol{k}} \times \overrightarrow{\boldsymbol{BP}} \tag{12}$$

where $\vec{\boldsymbol{k}}$ is a unit vector pointing in the positive z-axis direction. Since $\dot{\theta}_1$ is a passive variable, it should be eliminated from Eq.(12). To achieve this goal, we use the fact that the position vector of the rigid body rotating about a fixed point is normal to the velocity vector. We dot-multiply both sides of Eq.(12) by $\overrightarrow{\boldsymbol{AB}}$, which leads to

$$\overrightarrow{\boldsymbol{AB}} \bullet \dot{\overrightarrow{\boldsymbol{OP}}} = \dot{\theta}_2 \vec{\boldsymbol{k}} \bullet \left(\overrightarrow{\boldsymbol{BP}} \times \overrightarrow{\boldsymbol{AB}}\right) \tag{13}$$

Following the same procedure like Eq.(11),(12) and (13), for a left(**O→C→D→P**) sub-chain, yields

$$\overrightarrow{\boldsymbol{CD}} \bullet \dot{\overrightarrow{\boldsymbol{OP}}} = \dot{\theta}_4 \vec{\boldsymbol{k}} \bullet \left(\overrightarrow{\boldsymbol{DP}} \times \overrightarrow{\boldsymbol{CD}}\right) \tag{14}$$

Eq.(13) and (14) can be arranged in matrix form :

$$\boldsymbol{J}_{\boldsymbol{p}} \dot{\overrightarrow{\boldsymbol{OP}}} = \boldsymbol{J}_{\boldsymbol{\theta}} \dot{\vec{\boldsymbol{\theta}}}_{\boldsymbol{a}} \tag{15}$$

where,

$$\boldsymbol{J}_{\boldsymbol{\theta}} = \begin{bmatrix} \vec{\boldsymbol{k}} \bullet (\overrightarrow{\boldsymbol{BP}} \times \overrightarrow{\boldsymbol{AB}}) & 0 \\ 0 & \vec{\boldsymbol{k}} \bullet (\overrightarrow{\boldsymbol{DP}} \times \overrightarrow{\boldsymbol{CD}}) \end{bmatrix} = \begin{bmatrix} l_1 l_4 S_{1-2} & 0 \\ 0 & l_5 l_8 S_{3-4} \end{bmatrix}$$

$$\boldsymbol{J}_{\mathbf{p}} = \left[\overrightarrow{\boldsymbol{AB}} \quad \overrightarrow{\boldsymbol{CD}}\right]^{\mathbf{T}} = \begin{bmatrix} l_1 C_1 & l_1 S_1 \\ l_5 C_3 & l_5 S_3 \end{bmatrix},$$

$$S_{i-j} = sin(\theta_i - \theta_j)$$

$$C_{i-j} = cos(\theta_i - \theta_j)$$

3.3 Singularity Analysis

By using the vector method , we determine and analyze the singularities of the *Sensation*. By using the method, a great deal of physical insight into the singularity problem is gained, and it is possible to determine the workspace easily.

We also discuss the physical significance of each of the two types of singularities. Due to the existence of two Jacobian matrices, a parallel mechanism or manipulator is said to be at a singular configuration when either $\boldsymbol{J_\theta}$ or $\boldsymbol{J_p}$ or both are singular[14].

3.3.1 Direct Kinematic Singularities(DKS)

In the *Sensation*, direct kinematic singularities(DKS) arise when $\boldsymbol{J_p}$, in Eq.(15), is singular, i.e., Det($\boldsymbol{J_p}$) = 0 .

$$\left| \overrightarrow{\boldsymbol{AB}} \ \overrightarrow{\boldsymbol{CD}} \right| = 0 \tag{16}$$

Geomertrically, this means that the vector $\overrightarrow{\boldsymbol{AB}}$ parallels the vector $\overrightarrow{\boldsymbol{CD}}$ (Fig.3). Therefore, the vector $\overrightarrow{\boldsymbol{AB}}$ and $\overrightarrow{\boldsymbol{CD}}$ form a linearly dependent set of rank 1. This type of direct kinematic singuarity are shown in Fig.3.

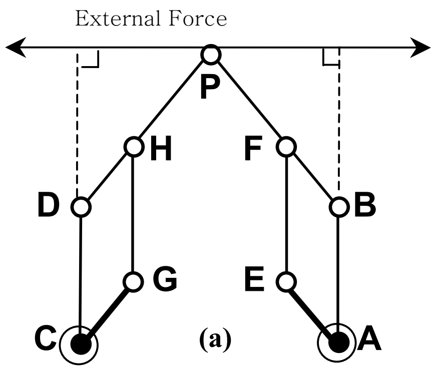

Figure 3. Direct kinematic singular configurations of the *SenSation*.

In Eq.(15), there exist some nonzero vector $\dot{\vec{\boldsymbol{P}}}$ vectors that result in zero $\dot{\vec{\boldsymbol{\theta}}}_{\boldsymbol{a}}$ vectors if $\boldsymbol{J_p}$ is singular. That is, the output **P** can possess infinitesimal motion in some direction while all the actuators are completely locked. Hence, the point **P** gains additional one degree of freedom and it cannot withstand external force along directions which are perpendicular to $\overrightarrow{\boldsymbol{AB}}$ (or $\overrightarrow{\boldsymbol{CD}}$) at **P** (see Fig.3.).

In typical parallel mechanism, direct kinematic singularities usually occur at the inside of the workspace and this is important one of the problems which typical parallel mechanisms have. For overcoming this singularity problem, the the Hexel machine have 8-motor for 5 axis use and Coline.C.L[17], S.J.Ryu and J.W.Kim and F.C.Park[4] have added actuators.

However, we overcame this problem by changing only the location of actuation whitout adding actuators because we design the *Sensation* so that the direct kinematic singularities(**DKS**) occur near the workspace boundary as shown in Fig.6. It is noticeable.

3.3.2 Inverse Kinematic Singularities(IKS)

Inverse kinematic singularities(IKS) of the *SenSation* occur when the determinant of $\boldsymbol{J_\theta}$ go to zero, i.e., Det($\boldsymbol{J_\theta}$) = 0.

$$\begin{vmatrix} \vec{k} \bullet (\overrightarrow{BP} \times \overrightarrow{AB}) & 0 \\ 0 & \vec{k} \bullet (\overrightarrow{DP} \times \overrightarrow{CD}) \end{vmatrix} = 0 \tag{17}$$

Geomertrically, this means that the vector $\overrightarrow{BP}$ parallels $\overrightarrow{AB}$ or $\overrightarrow{DP}$ parallels $\overrightarrow{CD}$. That is, any sub-chain is in a fully stretched-out or fold-back configuration. This type of inverse kinematic singuarities are shown in Fig.4.

When $\boldsymbol{J_\theta}$, in Eq.(15), is singular there exist some nonzero $\dot{\vec{\boldsymbol{\theta}}}_a$ vector that result in zero $\dot{\vec{\boldsymbol{P}}}$ vectors, i.e., infinitesimal rotation of the input link,AE and CG result in no output motion of joint **P**. Hence the *SenSation* loses one degree of freedom and can withstand external forces in directions along $\overline{\boldsymbol{PA}}$ or $\overline{\boldsymbol{PC}}$ without having actuator torques of joint A and C.

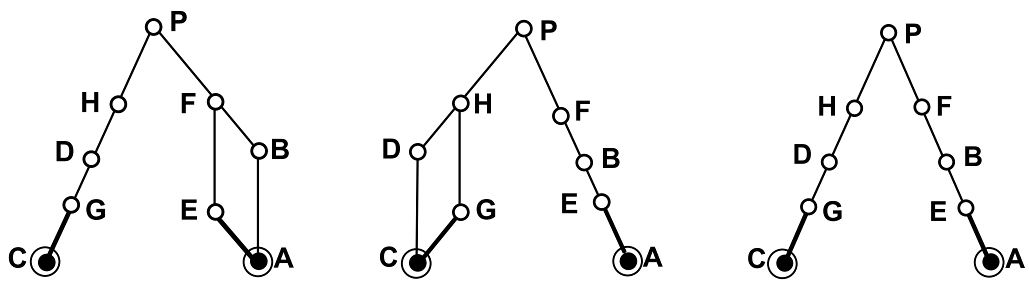

Figure 4. Inverse kinematic singular configurations of the the *SenSation*

In typical parallel mechanism, inverse kinematic singularities usually occur at the workspace boundary. Inverse kinematic singularities of the the *SenSation* also occur at the workspace boundary as shown in Fig.6.

4. Kinematic Performace

Since the workspace is separated by the direct kinematic singularities which occur at the inside of workspce, the workspace of typical parallel mechanisms is small in contrast to the link size.

To compare the singularty locus and workspace of the *SenSation* with those of the five-bar parallel mechanism[19], the direct kinematic singularity(DKS) and inverse kinematic singularity(IKS) loci of both five-bar parallel mechanism and the *SenSation* are shown in Fig.5 and 6 respectively.

Figure 5 represents the singularity and workspace of the five bar mechanism. The workspace is separated by DKS locus which occurr at the inside of workspace. Therefore one of the separated areas should be selected for tasks such as path planing.

However, we know that the direct kinematic singularitiy of the proposed mechanism occur near the boundary of workspace as shown in figure 6. Hence, we do not any more suffer from the direct kinematic singularities.

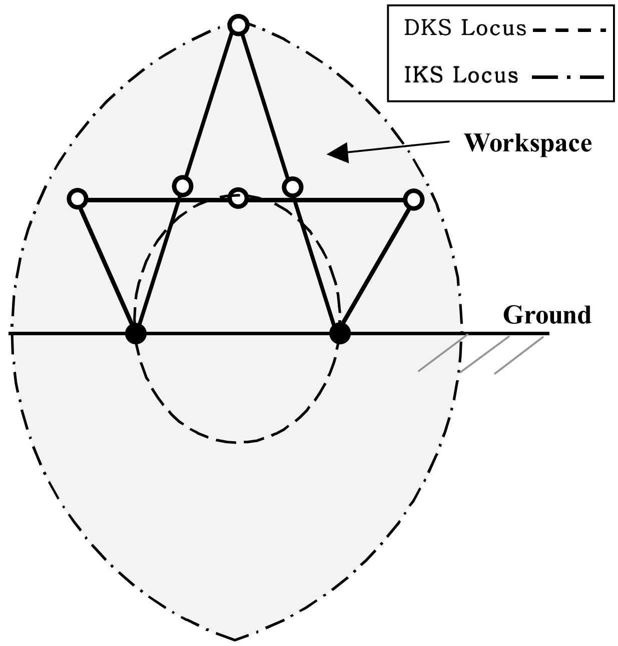

Figure 5. Singularity and workspace of the five-bar mechanism

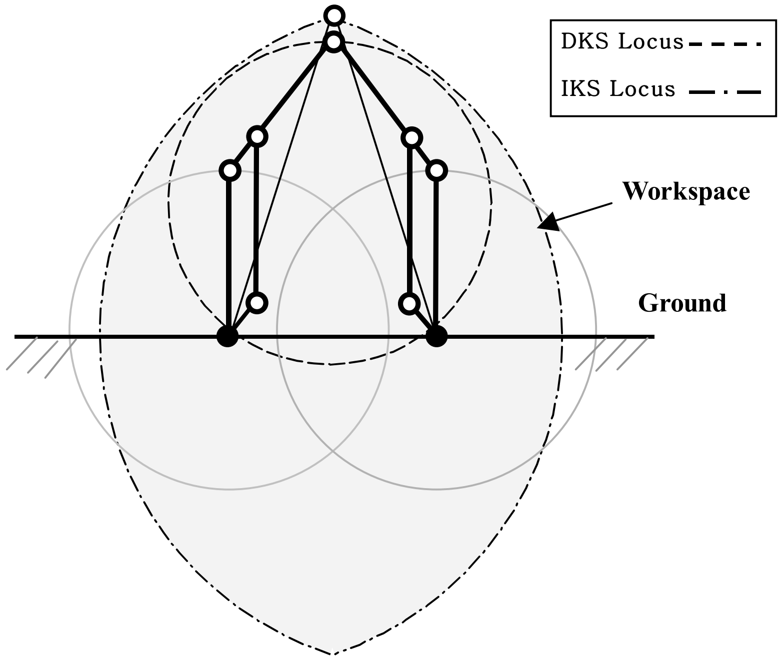

Figure 6. Singularity and workspace of the *SenSation*

To compare the kinematic performance of the the *SenSation* with that of five-bar parallel mechanism, the manipulablity ellipsoid is represented in Fig.7 and 8. We select the link parameters of two mechanism, $l_1 = l_5 = l_3 = l_7 = l_4 = l_8 = 0.18$ (m), $l_2 = l_6$, =0.3 (m), $\mathbf{d}$ = 0.18/2 (m) arbitrarily.

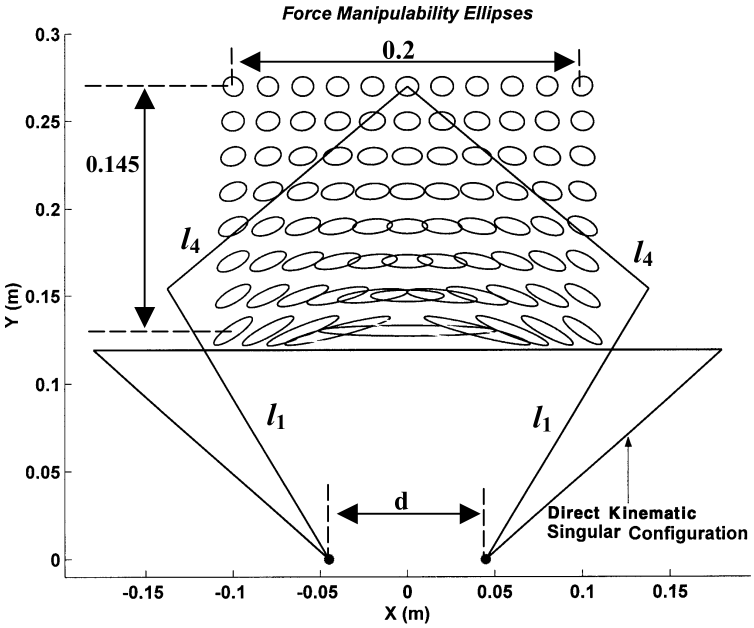

Figure.7 Manipulablility Ellipses of five-bar mechanism

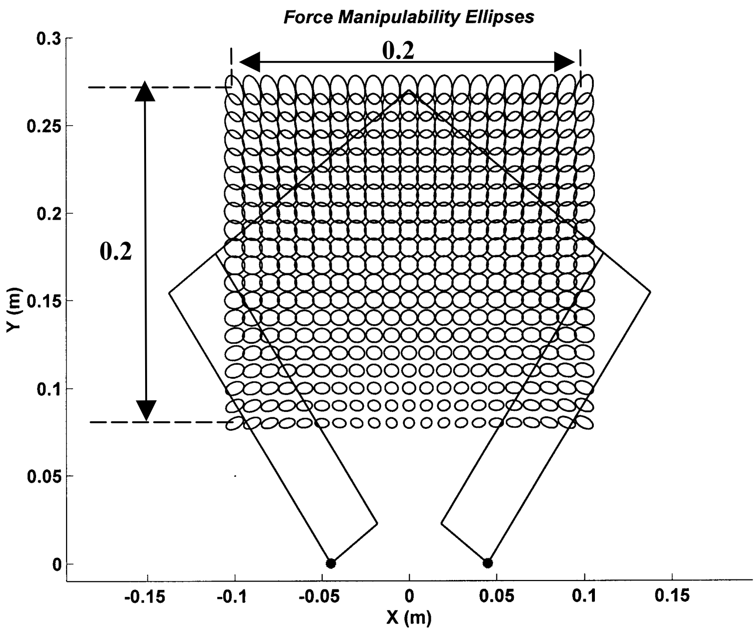

Figure.8 Manipulablility Ellipses of the the *SenSation*

The manipulability ellipses of the five-bar parallel mechanism is shown in Fig. 7. Because of the direct kinematic singulaties at inside of workspace(see Fig.7), the manipulablity ellipses is not good. In constrast to link size, it have a small workspace.

In the the *SenSation*, since there are the direct kinematic singularities near the boundary of workspace(see Fig.6), we know, comparing Fig.5 and 7 with Fig.6 and 8, that this mechanism have the workspace lager than those of five-bar parallel mechanism.

Especially, the improvement in manipulability ellipses from Fig. 7 to Fig. 8 is noticeable. Also, form Fig.8, we know that the *SenSation* have a good the kinematic isotropy through the entire workspace without optimization of the link parameters and adding actuators.

5. Static Balance

In the context of manipulators and motion simulation mechanisms, static balancing is defined as the set of conditions under which the weight of the links of the mechanism does not produce any torque at the actuators under static conditions, for any configuration of the mechanism[17][18]. A balanced mechanism results in better dynamic characteristics and less vibration caused by fast motion. We assume that $\boldsymbol{l}_1 = \boldsymbol{l}_5 = \boldsymbol{l}_3 = \boldsymbol{l}_7$, $\boldsymbol{l}_2 = \boldsymbol{l}_6$, $\boldsymbol{l}_4 = \boldsymbol{l}_8$. The potential energy of the *SenSation* can be written as

$$\begin{aligned} V = \sum m_i g L_{ci} = g\{ & m_1 l_{c1} S_1 + m_2 l_{c2} S_2 + m_3 (l_2 S_2 + l_{c3} S_1) + m_4 (l_1 S_1 + l_{c4} S_2) \\ & + m_1 l_{c1} S_3 + m_2 l_{c2} S_4 + m_3 (l_2 S_4 + l_{c3} S_3) + m_4 (l_1 S_3 + l_{c4} S_4)\} \end{aligned} \tag{18}$$

where m_i is the mass of each link and L_{ci} represents the position of the center of mass of each link.

Rearranging Eq.(18) yields,

$$V = g\{(m_1 l_{c1} + m_3 l_{c3} + m_4 l_1)(S_1 + S_3) + (m_2 l_{c2} + m_3 l_2 + m_4 l_{c4})(S_2 + S_4)\} \tag{19}$$

In equationq (19) if the coefficients of $(S_1 + S_3)$ and $(S_2 + S_4)$ go to zero, then the potential energy of the *SenSation* will be zero for any configuration. Hence, one obtains the conditions for static balancing as follows

$$\begin{aligned} (m_1 l_{c1} + m_3 l_{c3} + m_4 l_1) = 0 \\ (m_2 l_{c2} + m_3 l_2 + m_4 l_{c4}) = 0 \end{aligned} \tag{20}$$

For satisfying the condition of static balancing described in equation (20), we change the location of center of mass of link 1 and 2. Hence, the static balance of the S*enSation* can be achieved as shown in Fig.9.

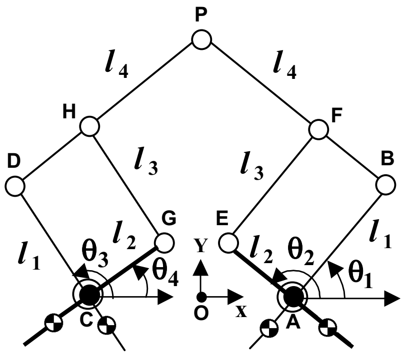

Figure 9. Static balance of the *SenSation*

Because the *SenSation* is statically balanced, the actuators are used only to transfer accelerations to the moving links, which leads to a reduction of size and power of the actuators and results in significant improvements of the control and energy efficiency. If the mechanism proposed is applied to the limbs of flight simulator, haptic device, machining center that has the parallel structure, they will have a good dynamic performance.

6. Conclusion

We proposed a new 2 DOF parallel mechanism, the *SenSation,* that has translational two degrees of freedom. The *SenSation* is designed inorder to have not only the global kinematic isotropy performance and static balance.

For the purpose of this kinematic performace, we changed the location of actuations by employing the pantograph mechanism, which result in the existence of direct kinematic singularity locus near the boundary of workspace as shown in Fig.6. Therefore, the *SenSation* overcame disadvantage such as the singular configurations existing in the inside of workspace for typical parallel mechanisms. Form Fig.8, we knew that the *SenSation* have a good the kinematic isotropy through the entire workspace without optimization of the link parameters and adding actuators.

For the purpose of static balance, we derived the condition of zero-potential energy and achieved the static balance by chaing the location of center of mass of links as shown in Fig.9.

7. Reference

[1] Gough V.E., 1956., “Contribution to discussion of papers on research in automotive stability, control and tyre performance.” Proc. Auto Div. Inst. Mechanical Engineers.

[2] Stewart D., 1965., “A platform with 6 degrees of freedom.” Proc. Of the Intitution of mechaniscal engineers, 180(part1, 15), pp.371-386.

[3] Clavel, R., 1988., “DELTA, a fast robot with parallel geometry.” Proc. Of 18th International Symp. On Industrial Robots., pp. 91-100.

[4] S.J.Ryu and J.W.Kim and F.C. Park., 1998, “Eclipse: An Overactuated Parallel Mechanism for Rapid Machining”, 1998 ASME International Mechanical Engineering Congress and Exposition, vol.8, pp.681-689.

[5] Tonshoff H.K., 1998, “Asystematic comparisom of parallel kinematics.” Keynote in Proc. Of the first European-American forum on parallel kinematic machines, Milan, Italy, Aug.31-Sep. 1,

[6] Pierrot F., Shibukawa T., 1998, "From Hexa to HexaM." In Proc. 1st PK'98 : International parallel kinematik-Kolloquium, pp.75-84.
[7] Pierrot F., Dauchez P. And Foumier A., 1991, " Fast parallel robots." Journal of Robotic Systems, Vol. 8, No.6, pp829-840.
[8] Pierrot F., 1999, " H4 : a new family of 4-dof parallel robots." Proc. Of IEEE/ASME, Intenational Conference on Advanced intelligent Mechatronics, pp.508-513.
[9] Hudgens,J.C.,and Tesar,d., 1988, "A Fully-Parallel Six Degree-of-freedom Micromanipulator: kinematic Analysis and Dynamic Model," Trends and Developments in Mechanisms, machines, and Robotics Proc. Of the 20th Biennial Mechanisms Conference, ASME, New York, De-Vol. 15-3, pp. 29-37.
[10] F.Tahmasebi., 1992, "Kinematic Synthesis and Analysis of a Novel Class of Six-DOF Parallel Minimanipulators," Ph.D thesis, University of Maryland., Dept. Of Mech. Eng and Institute for systems Research.
[11] Antonio Frisoli, and Giuseppe Maria Prisco,.etc., 1999, "A Novel Tehdon Driven 5-Bar Linkage With a Large Isotropic Workspace," Proc. Of the ASME Dynamic Systems and Control Division. pp. 297-304.
[12] Antonio Frisoli, Fabio Salsedo and Massimo Bergamasco (PERCRO, Scuola Superiore S. Anna – Pisa, Italy), 1999, "Design of a New Tendon Driven Haptic Interface with Six Degrees of Freedom." 8th International Workshop on Robot and Human Interaction.
[13] J.W.Kim and F.C.Park., 1998, "Manipulability of Closed kinematic Chain", ASME Journal of mechanical Design. Vol. 120, pp. 542-548,
[14] Gosselin, C. and Angeles, J., 1990, "Singularity Analysis of closed-Loop Kinematic Chain." IEEE Trans. On Robotics and Automation., Vol. 6, No.3, pp 281-290.
[15] R.E. Stamper., 1997, "A Three Degree of Freedom Parallel Mnipulator with Only Translation Degree of Freedom." Ph.D Thesis, University of Maryland., Dept. Of Mech. Eng and Institute for systems Research.
[16] Collins, C. L., 1997, "Singularity Analysis and Design of Parallel Manipulators", Ph.D Thesis, University of California, Irvine., Dept. of Mechanical and Aerospace Engineering.
[17] Gosselin, C. and Wang, J.,2000,. "Static Balancing of Spatial Six-Degree-of Freedom Parallel Mechanisms with Revolute Actuators." Journal of Robotic System., Vol.17., No.3., pp.159-170.
[18] I. Ebert-Uphoff and Gosselin, C. and T. Laliberte, 2000, "Static Balancing of Spatial Parallel Platform Mechanisms - Revisited", ASME Journal of Mechanical Design, Vol.122, No.1, pp. 43-51.
[19] Hayward. V, and Choksi. J., Lanvin. G. and Ramstein. C., 1994., "Design and multi-objective optimization of a linkage for a haptic interface.", Advances inRobot Kinemtics and Computationed Geometry, pp. 359-368. Kluwer Academic Publishers.
[20] Hunt, K. H., 1978, "*Kinematic Geometry of mechanisms.*" Oxford, UK., Oxford Science Publication.